RSC Advances

ROYAL SOCIETY OF CHEMISTRY

www.rsc.org/advances

Journal Name

COMMUNICATION

Targeted Design and Synthesis of a Highly Selective Mo-based Catalyst for the Synthesis of Higher Alcohols

Received 00th January 20xx,
Accepted 00th January 20xx

DOI: 10.1039/x0xx00000x

www.rsc.org/

Wei Xie,[a] Jilong Zhou,[a] Lili Ji,[a] Song Sun,*[ab] Haibin Pan,[a] Junfa Zhu,[a] Chen Gao,*[ab] and Jun Bao*[ab]

Improving the C_{2+} alcohols selectivity is the most difficult challenge in higher alcohol synthesis (HAS) from syngas. Herein, three effective strategies were combined to develop a Mo-based catalyst for HAS. The sol-gel method produced a highly homogeneous distribution of components, which ensured an intimate and sufficient contact between different active sites. The incorporation of Mn oxide enhanced the interaction between Co and Mo and thus promoting the growth of alcohol chain. More importantly, the reduction degrees of Co and Mo can be tuned precisely. The prepared Mn/K/Co/Mo catalysts show unusual activity for HAS.

In the last few decades, the catalytic conversion of syngas to higher (C_{2+}) alcohols has attracted significant research attention, owing to the relevance of higher alcohols as neat fuels, fuel additives and a feedstock for the synthesis of a variety of valuable chemicals.[1] The reaction is a typical example of those requiring synergetic effects between different catalytic sites with different functionality. Specifically, an active catalyst for the synthesis of higher alcohols from syngas should possess multiple active species corresponding to CO adsorption, dissociation, hydrogenation, and CO non-dissociative insertion etc., respectively.[2] Precise regulation of these active species to obtain a good synergy between each other is crucial to increase the catalyst activity. Due to this complex natures of the system, the development of solid catalysts displaying high selectivity for C_{2+} alcohols still remains the most attractive and difficult challenge and no commercial process exists today.

After decades of research, several catalyst families have been developed for producing alcohols from syngas.[3] Among these, Mo-based catalysts have drawn special interest due to their excellent sulfur tolerance.[4] Great efforts have been made to optimize the catalyst composition, regulate the catalyst structure and explore the structure-activity relationship as well as the reaction mechanism, etc.[2a,5] The addition of an alkali to a Mo catalyst increases alcohol production and suppresses hydrocarbon formation.[6] Some 3d transition metals, especially Co, are found to be effective promoters for improving the C_{2+} alcohol selectivity because they can promote the formation of alkyl group (C_nH_x), which is recognized as the key intermediate for the synthesis of higher alcohols.[7] Many factors, including the aggregation state of Mo species, the particle size, the interaction between promoters and Mo species, the reducibility of components as well as the distribution of different species etc. have significant influence on the catalytic performance.[4a,5d,8] Simultaneously tuning these structure factors to achieve the positive effects on catalyst performance is still very difficult. For instance, the $Mo^{\delta+}$ ($1<\delta<4$) species are regarded as the adsorption site for non-dissociative CO and responsible for alcohol formation.[2a,9] However, under the reduction condition for producing $Mo^{\delta+}$ ($1<\delta<4$) species, most of Co species were often over-reduced to metal Co^0, which was highly active for CO dissociative adsorption and hydrogenation and thus enhanced the hydrocarbons formation.

Herein, we combined three strategies to develop a highly efficient K and Co promoted Mo catalyst for the conversion of syngas to higher alcohols. First, a Mn oxide was introduced as the third promoter to tune the interaction between Co and Mo species, the reducibility of components as well as the aggregation state of Mo species based on the unique electronic and structural effects of Mn oxide. The related research has rarely been reported previously. Second, a modified sol-gel preparation method was employed to achieve a highly homogeneous distribution of components on the catalyst, ensuring an intimate and sufficient contact between promoters and Mo species. More importantly, a two-steps activation approach for catalyst activation was used to tune and match the reduction degree of Co and Mo species. Based on these targeted design, synthesis and activation strategies,

[a] National Synchrotron Radiation Laboratory, Collaborative Innovation Center of Chemistry for Energy Materials, University of Science and Technology of China, Hefei, Anhui 230029 (P. R. China). E-mail: suns@ustc.edu.cn, cgao@ustc.edu.cn, baoj@ustc.edu.cn.
[b] CAS Key Laboratory of Materials for Energy Conversion, Department of Materials Science and Engineering, University of Science and Technology of China, Hefei, Anhui 230026 (P. R. China).

† Electronic Supplementary Information (ESI) available: Experimental details and characterization. See DOI: 10.1039/x0xx00000x

the obtained Mn/K/Co/Mo catalyst showed unusual activity for higher alcohol synthesis from syngas.

The citric acid was used as a complexing agent during the sol-gel process for the preparation of catalyst. The as-prepared dried gel was heat-treated in nitrogen to form the fresh catalyst powder. The decomposition of citric acid in nitrogen atmosphere reduced the Mo species and meanwhile inhibited the growth of particle size. Before reaction, the catalyst underwent the second reduction step using pure H_2. XRD patterns (Fig. S1, ESI†) show that for the sample without Mn promoter, only three diffraction peaks at 2θ = 26.1°, 37.0° and 53.5° were observed, corresponding to the {-111}, {-211} and {-312} facets of MoO_2 crystalline. The formation of MoO_2 can be attributed to the reduction effect of the decomposition of citric acid in nitrogen atmosphere. The weak diffraction intensities indicated a low degree of crystallization. Besides it, no peaks assigned to other Mo or Co species were detected. The doping of Mn promoter led to a significant change in XRD patterns. At a low Mn/Mo ratio of 0.05, five new weak peaks appeared at 2θ values of 18.2°, 35.7°, 52.1°, 56.3° and 64.2°. They could be attributed to the poorly crystalline $CoMoO_3$ phases. When further increasing the Mn content, a series of new diffraction peaks assigned to $Co_2Mo_3O_8$ phase were observed. It can be seen that with an increase in the Mn content, the diffraction intensities of Co-Mo phases became stronger, while that of the MoO_2 decreased. The results indicated that the doping of Mn promoter significantly enhanced the interaction between Co and Mo species and improved the degree of crystallization. It is noted that no any peaks of Mn oxides were detected even at a relatively high Mn content, which may indicate that the Mn species were either amorphous or present in the form of very small nanoparticles with a high dispersion on the catalysts.

The morphology and microstructure of the catalysts were investigated by TEM technique. For the sample without Mn (Fig. S2a, ESI†), the large-size particles with irregular shape were the amorphous char, which was produced by the decomposition of citric acid in nitrogen. The catalyst particles had a size of about 5 nm and were homogeneously dispersed in the char. The pattern of electron diffraction further confirmed that the particle had an amorphous structure. After incorporating Mn promoter (Fig. S2b and S2c, ESI†) the catalyst particle had a regular plate-like structure, indicating a high degree of crystallization, which was further proved by the electron diffraction pattern. The clear and uniform lattice fringes observed in high-resolution TEM image (Fig. S3, ESI†) confirmed that the plate-like particles were highly crystallized $Co_2Mo_3O_8$, consistent with XRD results. The EDS mapping (Fig. S4, ESI†) indicated that the Co, Mo and Mn elements were distributed uniformly on the surface of the catalysts.

The distribution of Mo species of the catalysts derived from high-resolution X-ray photoelectron spectroscopy (Fig. S5, ESI†) are summarized (Table S1, ESI†). For the fresh Mn-free sample, besides the characteristic binding energies of Mo^{6+} $3d_{5/2}$ (232.4 eV) and Mo^{6+} $3d_{3/2}$ (235.6 eV), two new peaks assigned to Mo^{4+} $3d_{5/2}$ (230.6 eV) and Mo^{4+} $3d_{3/2}$ (233.8 eV) were also observed, indicating the formation of Mo^{4+}

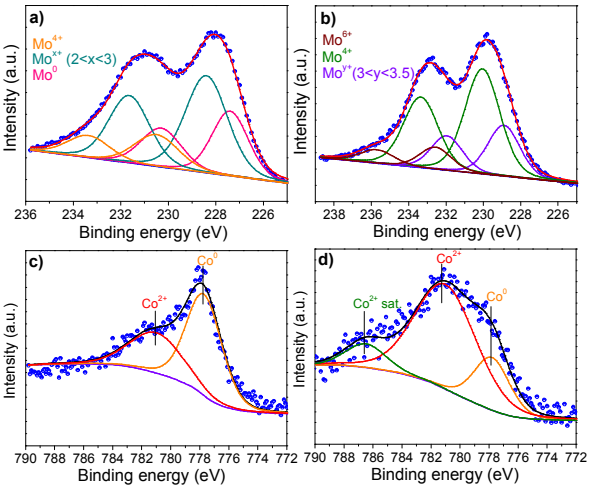

Fig. 1 In-situ synchrotron radiation XPS spectra of the reduced catalysts. a) Mo 3d spectra of Mn-free catalyst. b) Mo 3d spectra of Mn-doped catalyst with Mn/Mo ratio of 0.15. c) Co 2p spectra of Mn-free catalyst. d) Co 2p spectra of Mn-doped catalyst with Mn/Mo ratio of 0.15.

species.[9b] When incorporating the Mn promoter, the binding energies of Mo species did not change. However the surface content of Mo^{6+} species decreased whilst that of Mo^{4+} species increased significantly, indicating that the incorporation of Mn promoter promoted the reduction of Mo^{6+} to Mo^{4+} species during the decomposition of citric acid in nitrogen. The reason may be due to the fact that the doping of Mn facilitated the formation of two new phases $CoMoO_3$ and $Co_2Mo_3O_8$, in which the valence state of Mo was +4. From the Co 2p core-level spectra, the binding energy of 780.9 eV and satellite peak at 786.7 eV indicated the presence of Co^{2+} species in the fresh catalysts (Fig. S6, ESI†).[10] For the Mn-doped fresh sample, the appearance of binding energy of Mn $2p_{3/2}$ (641.2 eV) and Mn $2p_{1/2}$ (653.2 eV) confirmed the existence of Mn^{2+} species (Fig. S7, ESI†).[11] These results indicated that the decomposition of citric acid in nitrogen cannot reduce the Co and Mn species.

The in-situ synchrotron radiation XPS was employed for investigating the surface chemical compositions of the reduced catalysts. As shown in Fig. 1, after reduction in pure H_2 under 673 K, new Mo species with lower valence state were formed on the surface of catalysts. For the catalyst without Mn, besides the Mo^{4+}, the peaks at 227.4 eV and 228.4 eV can be attributed to the metal Mo^0 and Mo^{x+} (2<x<3) species, respectively.[12] After incorporating with Mn, a new peak at 228.9 eV was observed, corresponding to the Mo phase with a valence state of +y (3<y<3.5),[12] higher than that of the Mo^{x+} (2<x<3) species. Besides it, no peak assigned to metallic state Mo was observed on the reduced Mn-doped catalyst. These results demonstrated that the presence of Mn inhibited the reduction of Mo^{4+} species during the H_2 treatment. From the Co 2p spectra, it is evident that after reduction a large amount of metallic state Co^0 (Co $2p_{3/2}$ peak at 777.9 eV) were formed on the sample without Mn.[10,13] The Mn-doped catalyst exhibited a rather broad Co $2p_{3/2}$ peak at about 781.0 eV, which suggested the coexistence of several oxidation states,

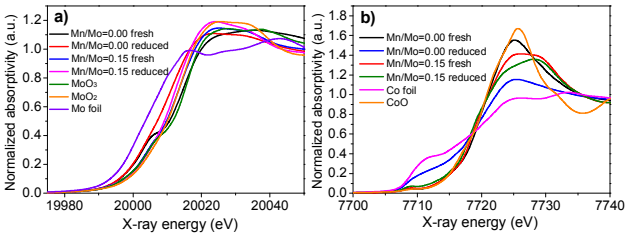

Fig. 2 a) Mo K-edge and b) Co K-edge XANES spectra of the catalysts.

predominantly Co^{2+} and some Co^0.[13] Compared with the Mn-free catalyst, the fraction of metallic Co^0 decreased significantly when Mn was added, indicating that the reducibility of Co species was also suppressed by the addition of Mn. The chemical state of Mn species did not changed significantly after reduction (Fig. S8, ESI†).

The normalized Mo K-edge XANES spectra of the fresh and reduced catalysts and two standard compounds MoO_3 and MoO_2 are shown in Fig. 2a. The absorption edge position provides the information about the chemical valence of central metal atoms, and the pre-edge peak intensity is sensitive to the symmetry of the absorbing atom.[14] The fresh Mn-free catalyst exhibited an obvious pre-edge peak higher than that of MoO_3, indicating that the central Mo atoms existed in not only octahedral but also tetrahedral coordination. The absorption edge energy was lower than that of MoO_3. The reason was attributed to the formation of MoO_2 species, as revealed by XRD results. After reduction, the pre-edge peak disappeared completely, suggesting that the Mo atoms in reduced sample had a strictly octahedral field. The 1s→4d transition was forbidden in the octahedral symmetry. The absorption edge was shifted to lower value than that of MoO_2, which indicated that the H_2 reduction resulted in the formation of lower valence state of Mo species, consistent with the in-situ XPS results. The fresh Mn-doped sample had lower absorption edge energy as compared to the Mn-free sample due to the incorporation of Mn promoting the reduction of Mo^{6+} during the decomposition of citric acid. After reduction in pure H_2, the absorption edge position was shifted to lower value, but higher than that of the reduced Mn-free sample because the presence of Mn inhibited the reduction of Mo species during the H_2 treatment. Furthermore, no pre-edge peak was observed for the Mn-doped samples, suggesting that the Mo atoms were mainly present in octahedral coordination. The Co K-edge XANES spectra of the undoped and doped catalysts are shown in Fig. 2b. The fresh undoped sample had similar absorption edge energy as that of CoO. After reduction, the absorption edge shifted to lower value, close to that of Co foil, indicating the formation of metal Co^0. For the Mn-doped sample, the position of absorption edge did not show obvious change, suggesting the reduction of Co was inhibited.

The catalytic performance of the catalysts for the synthesis of higher alcohols was tested under the conditions of

Table 1. CO hydrogenation over the catalysts as a function of Mn contents.[a,b,c]

Sample (Mn/Mo)	CO. conv. (%)	Alc. Sel. (%)	C_{2+}/C_1	Alc. STY. (g/kg/h)
0.00	40.2	4.2	0.4	14.7
0.05	30.8	21.1	1.5	63.2
0.10	21.5	53.1	3.5	85.7
0.15	24.0	51.6	3.8	91.4
0.20	19.7	50.1	3.9	78.3
0.25	17.4	55.8	5.2	68.2

[a] Catalysts: K/Mo=0.1, Co/Mo=0.5. [b] Reduction conditions: catalyst 0.5 g, T=673 K, pure H_2; reaction conditions: P= 5.0 MPa, T=573 K, GHSV=4800 h^{-1}, H_2/CO=2. [c] Conv.=conversion, Alc.Sel.=alcohols selectivity, Alc.STY.= space-time-yield of alcohols. Both CO conversion and alcohols selectivity are calculated on a CO_2-free basis. C_{2+}OH/MeOH is based on moles of carbon.

5.0 MPa, 573 K, 4800 h^{-1}, and a H_2 to CO molar ratio of 2. Table 1 lists the activity data after an induction period of 24 h. Over the Mn-free catalyst, the CO conversion was relatively high, while the space-time-yield (STY) and selectivity toward alcohol synthesis were extremely low. The predominant product was hydrocarbon. When Mn was incorporated as a promoter, the alcohol selectivity and STY significantly increased although the CO conversion decreased. The catalyst with a Mn/Mo molar ratio of 0.15 exhibited the best performance for alcohol synthesis. On this catalyst, the STY of total alcohol was 91.4 $g \cdot kg^{-1} \cdot h^{-1}$, approximately 6.2 times as high as that of the Mn-free sample. Especially, the selectivity to alcohol increased sharply from 4.2% to 51.6%. The alcohol product distributions are present in Fig. 3a. For the Mn-free catalyst, the alcohol product distribution obeyed the Anderson-Schulz-Flory (ASF) law and the methanol was the predominant alcohol. The Mn-doped catalysts gave a completely different alcohol product distribution as the product distribution deviated from the ASF law. The formation of methanol was significantly suppressed and the ethanol became the predominant product. The effect of reaction temperature on the catalytic performance over the catalyst with Mn/Mo ratio of 0.15 was listed in Table 2. At a reaction temperature of 593 K, the catalyst showed the best activity. The total alcohol STY reached 148.3 $g \cdot kg^{-1} \cdot h^{-1}$ with a high selectivity of 58.6%.

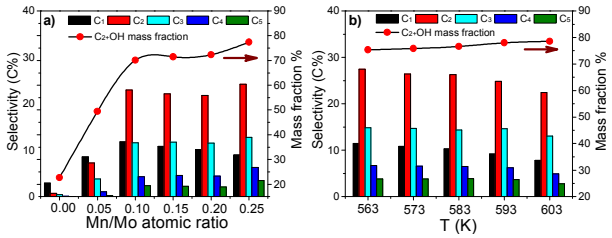

Fig. 3 Alcohol products distribution on a) the catalysts with different Mn/Mo ratios. b) the catalyst with Mn/Mo ratio of 0.15 under different reaction temperature.

Table 2. Effect of reaction temperature on the catalytic performance of the Mn-promoted catalyst.[a,b,c]

T (K)	CO. conv. (%)	Alc. Sel. (%)	C_{2+}/C_1	Alc. STY. (g/kg/h)
563	9.3	64.3	4.6	57.8
573	15.0	62.4	4.8	94.1
583	18.9	61.4	5.0	124.9
593	23.9	58.6	5.4	148.3
603	26.1	51.0	5.5	133.0

[a] Catalysts: K/Mo=0.115, Co/Mo=0.5, Mn/Mo=0.15. [b] Reduction conditions: catalyst 0.5 g, T=723 K, pure H_2; reaction conditions: P= 5.0 MPa, GHSV=6000 h^{-1}, H_2/CO=2. [c] Conv.=conversion, Alc.Sel.=alcohols selectivity, Alc.STY.= space-time-yield of alcohols. Both CO conversion and alcohols selectivity are calculated on a CO_2-free basis. C_{2+}OH/MeOH is based on moles of carbon.

Furthermore, the ratio of C_{2+}OH/MeOH increased to 5.4. The mass fraction of C_{2+}OH in the total alcohols approached 80% (Fig. 3b). To our best knowledge, the selectivity to C_{2+}OH in total alcohol is the highest value achieved to date for Mo-based catalyst system.

For the Mo-based catalyst, the methanol is directly formed by the hydrogenation of non-dissociatively adsorbed CO, while the higher alcohols are generally formed via a CO insertion mechanism.[2a,2b,15] First, the adsorbed CO was dissociated and then hydrogenated to form CH_2, followed by the growth of the alkyl chain via CH_2 insertion. Then the non-dissociatively adsorbed CO inserted into an alkyl group to form an acyl species, which was hydrogenated to the corresponding alcohol or to a longer alkyl group via CH_2 insertion. The hydrocarbons were produced by the hydrogenation of the alkyl groups. For the activated Co-Mo catalyst, the $Mo^{\delta+}$ ($1<\delta<4$) species are the main adsorption site for non-dissociative CO and favors the CO insertion into alkyl species to produce alcohol, while the metal Co^0 and metal Mo^0 are highly active for hydrogenation. Too strong hydrogenation ability is conducive to the formation of hydrocarbons and thus inhibiting the synthesis of higher alcohols.

From the characterization results, the incorporation of Mn oxide combining the two-steps activation approach tuned the reduction degrees of Co and Mo species and optimized the distribution of different active sites. During the process of decomposition of citric acid in nitrogen, the incorporation of Mn promoted the reduction of Mo^{6+} to Mo^{4+}, whilst the Co species remained in the +2 oxidation state. In the second stage of H_2-reduction, the presence of Mn conversely suppressed the reduction of Mo^{4+} to metal Mo0, leading to the enrichment of $Mo^{\delta+}$ ($1<\delta<4$) species. The transformation of Co^{2+} to metal Co0 was also suppressed to some extent by the addition of Mn. Consequently, the strong capabilities for hydrogenation were inhibited reasonably, and meanwhile the CO insertion ability was enhanced significantly. The good synergies between CO dissociation, hydrogenation and CO insertion played a crucial role in the formation of higher alcohols and growth of carbon chain. Second, the strong interaction between Co and Mo species caused by the addition of Mn was suggested to enhance the promotion effect of Co for the growth of alcohol chain as well as alcohol production because the presence of Co is conducive to the formation of intermediate alkyl group.[7,16] Furthermore, the highly homogeneous distribution of components, derived from the sol-gel method, ensured an intimate and sufficient contact between different active sites and thus made it easier for the migration of reaction intermediates from one site to another, such as the migration of alkyl species from Co to Mo species for further CO insertion. These results demonstrated that by combining these strategies, some key structural properties of Mo-based catalyst for HAS can be tuned simultaneously to exert positive impact on the catalytic performance and thus improve significantly the selectivity to higher alcohols.

In summary, we demonstrated that the combined three strategies, related to design, synthesis and activation, respectively, are very effective for developing a Mo-based catalyst for higher alcohol synthesis from syngas. The catalyst, derived from these strategies, had a highly homogeneous distribution of components, strong interaction between promoters and Mo species, and especially the tuned reducibility of Co and Mo. These structural characteristics, to a large extent, promoted the formation of active sites and ensured good synergies between different active sites with different functionality. Benefited from this, the catalyst exhibited a very high selectivity for C_{2+} alcohol formation. The work offers a successful example of targeted design and synthesis of complex multifunctional catalysts.

This work was supported by the National Nature Science Foundation of China (11179034, 11205159), National Basic Research Program of China (973 Program, 2012CB922004).

Notes and references

1 (a) Y. Z. Xiang, V. Chitry, P. Liddicoat, P. Felfer, S. Ringer and N. Kruse, *J. Am. Chem. Soc.,* 2013, **135**, 7114-7117; (b) J. J. Spivey and A. Egbebi, *Chem. Soc. Rev.,* 2007, **36**, 1514-1528; (c) M. Gupta, M. L. Smith and J. J. Spivey, *ACS Catal.,* 2011, **1**, 641-656; (d) R. G. Herman, *Catal. Today,* 2000, **55**, 233-245.

2 (a) A. Muramatsu, T. Tatsumi and H. Tominaga, *J. Phys. Chem.,* 1992, **96**, 1334-1340; (b) T. Toyoda, T. Minami and E. W. Qian, *Energy Fuels,* 2013, **27**, 3769-3777; (c) R. M. Palomino, J. W. Magee, J. Llorca, S. D. Senanayake and M. G. White, *J. Catal.*, 2015, **329**, 87-94; (d) Y. W. Lu, F. Yu, J. Hu and J. Liu, *Appl. Catal., A,* 2012, **429-430**, 48-58; (e) K. G. Fang, D. B. Li, M. G. Lin, M. L. Xiang, W. Wei and Y. H. Sun, *Catal. Today,* 2009, **147**, 133-138.

3 (a) V. Subramani and S. K. Gangwal, *Energy Fuels,* 2008, **22**, 814-839; (b) V. R. Surisetty, A. K. Dalai and J. Kozinski, *Appl. Catal., A,* 2011, **404**, 1-11.

4 (a) M. R. Morrill, N. Tien-Thao, H. Shou, R. J. Davis, D. G. Barton, D. Ferrari, P. K. Agrawal and C. W. Jones, *ACS Catal*,,. 2013, **3**, 1665-1675; (b) S. Zaman and K. J. Smith, *Cat. Rev. Sci. Eng.*, 2012, **54**, 41-132.

5 (a) V. P. Santos, B. van der Linden, A. Chojecki, G. Budroni, S. Corthals, H. Shibata, G. R. Meima, F. Kapteijn, M. Makkee and G. Gascon, *ACS Catal*., 2013, **3**, 1634-1637; (b) H. Shou and R. J. Davis, *J. Catal.,* 2011, **282**, 83-93; (c) Z. R. Li, Y. L. Fu, M. Jiang, T. D. Hu, T. Liu and Y. N. Xie, *J. Catal.*, 2001, **199**, 155-161; (d) Y. Avila, C. Kappenstein, S. Pronier and J. Barrault, *Appl. Catal., A,* 1995, **132**, 97-109.

6 (a) H. C. Woo, I.-S. Nam, J. S. Lee, J. S. Chung and Y. G. Kim, *J. Catal.,* 1993, **142**, 672-690; (b) J. S. Lee, S. Kim, K. H. Lee, I.-S. Nam, J. S. Chung, Y. G. Kim and H. C. Woo, *Appl. Catal., A,* 1994, **110**, 11-25.

7 (a) D. A. Storm, *Top. Catal.,* 1995, **2**, 91-101; (b) Z. R. Li, Y. L. Fu, J. Bao, M. Jiang, T. D. Hu, T. Liu and Y. N. Xie, *Appl. Catal., A,* 2001, **220**, 21-30; (c) K. Y. Yin, H. Shou, D. Ferrari, C. W. Jones and R. J. Davis, *Top. Catal.,* 2013, **56**, 1740-1751.

8 (a) M. Jiang, G. Z. Bian and Y. L. Fu, *J. Catal.,* 1994, **146**, 144-154; (b) M. T. Claure, S. H. Chai, S. Dai, K. A. Unocic, F. M. Alamgir, P. K. Agrawal and C. W. Jones, *J. Catal.,* 2015, **324**, 88-97; (c) Y. Yang, Y. D. Wang, S. Liu, Q. Y. Song, Z. K. Xie and Z. Gao, *Catal. Lett.,* 2009, **127**, 448-455; (d) E. T. Liakakou, E. Heracleous, K. S. Triantafyllidis and A. A. Lemonidou, *Appl. Catal., B,* 2015, **165**, 296-305. (e) J. Bao, Y. L. Fu and G. Z. Bian, *Catal. Lett.,* 2008, **121**, 151-157.

9 (a) M. M. Zhang, W. Zhang, W. Xie, Z. M. Qi, G. M. Wu, M. M. Lv, S. Sun and J. Bao, *J. Mol. Catal. A: Chem.,* 2014, **395**, 269-275; (b) M. M. Lv, W. Xie, S. Sun, G. M. Wu, L. R. Zheng, S. Q. Chu, C. Gao and J. Bao, *Catal. Sci. Technol.,* 2015, **5**, 2925-2934; (c) X. G. Li, L. J. Feng, LL. J. Zhang, D. B. Dadyburjor and E. L. Kugler, *Molecules,* 2003, **8**, 13-20.

10 S. S.-Y. Lin, D. H. Kim, M. H. Engelhard and S. Y. Ha, *J. Catal.,* 2010, **273**, 229-235.

11 (a) Y. M. Sun, X. L. Hu, W. Luo and Y. H. Huang, *J. Mater. Chem.,* 2012, **22**, 19190-19195; (b) D. P. Dubal, D. S. Dhawale, R. R. Salunkhe and C. D. Lokhande, *J. Electroanal. Chem.,* 2010, **647**, 60-65.

12 O. Marin-Flores, L. Scudiero and S. Ha, *Surf. Sci.,* 2009, **603**, 2327-2332.

13 L. Ovari, S. K. Calderon, Y. Lykhach, J. Libuda, A. Erdohelyi, C. Papp, J. Kiss and H. P. Steinruck, *J. Catal.,* 2013, **307**, 132-139.

14 F. de groot, *Chem. Rev.,* 2001, **101**, 1779-1808.

15 (a) K. J. Smith, R. G. Herman and K. Kier, Chem. Eng. Sci. 1990, **45**, 2639-2646; (b) T. Y. Park, I. Nam and Y. G. Kim, *Ind. Eng. Chem. Res.,* 1997, 36, 5246-5257.

16 (a) G. Z. Bian, Y. L. Fu and Y. S. Ma, *Catal. Today,* 1999, **51**, 187-193; (b) M. L. Xiang, D. B. Li, W. H. Li, B. Zhong and Y H. Sun, *Catal. Commun.,* 2007, **8**, 503-507.

Graphical Abstract

Three effective strategies were combined to develop a Mo-based catalyst for higher alcohol synthesis. The catalyst had good synergies between different active sites with different functionality. Benefited from this, the catalyst exhibited a very high selectivity for C_{2+} alcohol formation.